Soliton generation by long-wave short-wave interaction on the finite interval

2001 J. Phys. A: Math. Gen. 34 117

(http://iopscience.iop.org/0305-4470/34/1/309)

INSTITUTE OF PHYSICS PUBLISHING JOURNAL OF PHYSICS A: MATHEMATICAL AND GENERAL

J. Phys. A: Math. Gen. **34** (2001) 117–127 www.iop.org/Journals/ja PII: S0305-4470(01)17070-8

Soliton generation by long-wave short-wave interaction on the finite interval

F-X Hugot and J Leon

Physique Mathématique et Théorique, Université Montpellier 2, CNRS-UMR5825, 34095 Montpellier, Cedex 05, France

Received 11 September 2000

Abstract

The Karpman–Kaup equation is a generic limit model for one-dimensional long-wave short-wave resonant interaction within the Benney criterion. We show that (1) the input short-wave fields generate solitons, (2) the boundary inputs allow one to drive the soliton, (3) the spectral transform tool can be adapted to solve (linearize) the finite-interval problem and (4) the explicit solution provided by the semi-infinite interval limit produces a very accurate description of the finite-interval case. The argumentation is based on the solution of this equation by the inverse spectral transform and the results are obtained by numerical simulation of both the original system and its spectral transform. The main issue is the demonstration that the spectral transform is a quite practical and efficient tool and that it has in this case a simple and explicit expression in terms of the input and output short-wave field values.

PACS number: 0340K

1. Introduction

Interaction of radiation with matter is a fundamental process in physics, used to study both matter and radiation, of relevance in various fields like nonlinear optics, plasma waves, light absorption in crystals, etc. A common feature of such processes is, in the classical situation, a basic model which generally consists of a Maxwell equation for the radiation coupled to a wave equation for the material excitation (Bloch equations, Navier–Stokes equations, etc). Before coming to our concern, we list a few of those basic models.

In a two-component cold ion plasma, the wave equations [1]

$$\begin{aligned} &\mathcal{E}_{tt} - 3v_{Te}^2\mathcal{E}_{xx} = -\omega_{pe}^2\frac{n}{n_0}\mathcal{E} \\ &n_{tt} - c_s^2 n_{xx} = \frac{1}{2}\frac{Ze^2}{m_i m_e \omega^2}(|E|^2)_{xx} \end{aligned} \tag{1.1}$$

couple a longitudinal electric field $\mathcal{E} = E\mathrm{e}^{\mathrm{i}\omega t} + \text{c.c.}$ (Langmuir wave) with the ion-acoustic density profile n_e (obeying Navier–Stokes equations) through the ponderomotive force. In

0305-4470/01/010117+11$30.00

that context, a celebrated reduced model for the slowly varying envelope E is the Zakharov equation (dimensionless) [2]

$$\begin{aligned} &\mathrm{i}E_t + E_{xx} = nE \\ &n_{tt} - n_{xx} = (|E|^2)_{xx}. \end{aligned} \tag{1.2}$$

In a one-dimensional chain of hydrogen-bonded molecules, the Davydov model [3]

$$\begin{aligned} &\mathrm{i}\hbar\dot{\phi}_n + J(\phi_{n+1} + \phi_{n-1} - 2\phi_n) = u_n\phi_n \\ &\ddot{u}_n - v_p^2(u_{n+1} - 2u_n + u_{n-1}) = \chi^2(|\phi_{n+1}|^2 + |\phi_{n-1}|^2 - 2|\phi_n|^2) \end{aligned} \tag{1.3}$$

couples the C=O stretching mode ϕ_n to the acoustic wave u_n along the hydrogen bond (actually the acoustic wave is β_n where $u_n = \chi(\beta_{n+1} - \beta_n)$). An analogous model in continuous variables is the Takeno equation [4]

$$\begin{aligned} &q_{tt} - c^2 q_{xx} + \omega_0^2 q = -\alpha u_x q \\ &u_{tt} - v^2 u_{xx} = \beta q_x q. \end{aligned} \tag{1.4}$$

In nonlinear optics, the Yariv model [5]

$$\begin{aligned} &X_{tt} + \omega_V^2 X = \epsilon_0 \alpha_0' \boldsymbol{E} \cdot \boldsymbol{E} \\ &c^2 \boldsymbol{E}_{xx} - \eta^2 \boldsymbol{E}_{tt} = N\alpha_0'(X\boldsymbol{E})_{tt} \end{aligned} \tag{1.5}$$

couples laser radiation (the electric field $\boldsymbol{E}$) with a collection of harmonic oscillators X through the dependence of the refractive index on X (case of non-zero differential polarizability α_0').

For such coupled wave equations one is interested in particular resonant interaction properties, depending on the considered physical situation. Generically, elementary resonant process result from the Brillouin selection rules

$$\omega_1 - \omega_2 = \Omega \qquad k_1 - k_2 = K \tag{1.6}$$

where ω_1 and ω_2 are the frequencies of two components of the *light* fields (electrostatic wave in (1.1), infrared radiation in (1.3) and lasers in (1.5)), and where Ω is the frequency of the medium excitation.

Following Benney [6], we are interested in the two-wave interaction process and look for the limit $k_1 \to k_2$ obtained in the case $K \ll k_1$. This means that we consider the resonant interaction of a *short-wave* $k = k_1$ with the *long-wave* K. In that situation, the Brillouin selection rules are mapped into the Benney criterion [6]

$$\frac{\partial\omega}{\partial k} = \frac{\Omega}{K} \tag{1.7}$$

which tells us that the two-wave resonant interaction takes place when the group velocity of the short-wave equals the phase velocity of the long-wave.

Applying this condition to the above coupled systems by means of the method of multiple scales, we obtain systematically [7, 8] the Karpman limit [9] which in reduced units and dimensions reads in the rest frame of the acoustic wave

$$q_t = -\tfrac{1}{2}(|u|^2)_x \qquad u_{xx} + (k^2 - q)u = 0. \tag{1.8}$$

The parameter k is defined from the chosen physical context and usually has positive real values (for instance in plasma, k measures the relative difference between the frequency of the applied electric field and the plasma electron frequency). Here $u(k, x, t)$ is the envelope of the short-wave which enters the medium in $x = 0$ and for which the following boundary values are prescribed:

$$u(k, 0, t) = a(k, t) \qquad u_x(k, 0, t) = b(k, t). \tag{1.9}$$

The real-valued function $q(x,t)$ denotes the long-wave envelope and the initial state of the medium is given by the datum

$$q(x,0) = Q(x). \tag{1.10}$$

The medium extending from $x = 0$ to L, the problem we are interested in is the evaluation of the output field value $u(k,L,t)$. To obtain the solution analytically, it is convenient to regularize the above system in the region of large L by assuming the Kaup generalization [10]

$$q_t = -\tfrac{1}{2}\int \mathrm{d}k\,(|u|^2)_x \qquad u_{xx} + (k^2 - q)u = 0 \tag{1.11}$$

which we shall call the Karpman–Kaup system. This generalization can be understood as describing the co-operative effects of all components (labelled by k) of an incoming wavepacket. For the case of a plasma, the derivation of the above system is displayed in the appendix of [7].

Our purpose here is first to demonstrate that the solution of the Karpman–Kaup system provided by the inverse spectral transform (IST) on the semi-line in [7] furnishes a very accurate solution to the finite-line case (relative precision of order 10^{-3}). This is done by numerical integration of the system and comparison with the analytical expression given in [7]. In doing this we will discover that the expressions of the (given) input field data and the (measured) output fields permit the explicit construction of the spectral transform. Hence, we also compare the found numerical spectral transform with the theoretical one (and find excellent agreement).

Second, we will show that the freedom of the boundary values (input data) allows one to drive in a rather arbitrary manner a soliton initially present in the medium. This will be done by using as input external fields, wavepackets with frequency in the forbidden band of the medium (e.g. below the plasma frequency) hence showing that a nonlinear structure (the soliton) permits energy transmission within the forbidden band (or phonon gap) as predicted in [9].

Finally, we shall display in appendix A the time evolution of the spectral transform and in appendix B the IST solution on the finite interval.

2. Soliton generation: theory

The Karpman–Kaup system, with initial-value problem on the semi-infinite line, that is to say

$$q_t = -\tfrac{1}{2}\int \mathrm{d}k\,(|u|^2)_x \qquad u_{xx} + (k^2 - q)u = 0 \tag{2.1}$$

$$x \in [0,\infty] : q(x,0) = Q(x) \tag{2.2}$$

and with the input boundary values

$$u(k,x,t)|_{x=0} = a(k,t) \qquad u_x(k,x,t)|_{x=0} = b(k,t) \tag{2.3}$$

has an explicit output solution

$$u(k,x,t)|_{x\to\infty} \sim U(k,t)\mathrm{e}^{\mathrm{i}kx} + V(k,t)\mathrm{e}^{-\mathrm{i}kx} \tag{2.4}$$

given in [7] and recalled for completeness in appendix A. This solution allows us to construct the *spectral transform* $\rho(k,t)$, also called the reflection coefficient, by

$$\rho = -\frac{\overline{V}B - U\overline{A}}{\overline{V}A - U\overline{B}} \tag{2.5}$$

under the condition that[1]

$$|A|^2 - |B|^2 \neq 0 \tag{2.6}$$

[1] If $|A| = |B|$ the output data U and V are not sufficient to construct the spectral transform ρ which then has to be constructed with the IST machinery as in [7].

where $A(k,t)$ and $B(k,t)$ are given from the input $a(k,t)$ and $b(k,t)$ by

$$A = \frac{1}{2}\left(a - \frac{b}{\mathrm{i}k}\right) \qquad B = \frac{1}{2}\left(a + \frac{b}{\mathrm{i}k}\right). \tag{2.7}$$

From the scattering theory, the function $\rho(k,t)$ contains the complete information on the spectral properties of the solution. In particular, the poles in the complex lower half k-plane are the spectral signature of the solitons while the real-k continuous spectrum is related to the radiation component of the solution. As in the present situation the poles are allowed to move in time, they can in particular move from the upper half-plane where they stand for resonances, to the lower half-plane where they become solitons.

To see this in a concrete example, we have solved in the appendix the time evolution of the spectral transform $\rho(k,t)$ for the following input:

$$u(k,x,t)|_{x=0} = g(k)a(t) \qquad u_x(k,x,t)|_{x=0} = \mathrm{i}kg(k)\frac{a(t)}{\gamma} \tag{2.8}$$

where the pulse shape $a(t)$ is a real-valued localized function, where the spectral distribution $g(k)$ is a localized smooth function of k and where the real constant $\gamma < 1$. The result is

$$\rho(k,t) = S\left(1 + \frac{4kR}{(H - 4k^2G - 2kR) - (H - 4k^2G + 2kR)\mathrm{e}^{-\mathrm{i}RT(t)}}\right) \tag{2.9}$$

with the following definitions:

$$G(k) = \frac{1}{4k}\int \frac{|g(\lambda)|^2\,\mathrm{d}\lambda}{\lambda - k + \mathrm{i}0} \qquad H(k) = \frac{1}{2k}\frac{\gamma^2 - 1}{\gamma^2}\int \frac{\lambda^2|g(\lambda)|^2\,\mathrm{d}\lambda}{\lambda - k + \mathrm{i}0} \tag{2.10}$$

$$S(k) = \frac{H - 4k^2G - 2kR}{H} \qquad R(k) = \sqrt{2G(2k^2G - H)} \tag{2.11}$$

$$T(t) = \int_0^t a^2(\tau)\,\mathrm{d}\tau. \tag{2.12}$$

The poles of the above expression in the lower half-plane are related to the soliton component of the solution. The motion of these poles are found by solving

$$\mathrm{e}^{-\mathrm{i}RT} = \frac{H - 4k^2G - 2kR}{H - 4k^2G + 2kR}. \tag{2.13}$$

It is remarkable that $H(k)$ and $G(k)$ (remember $\gamma < 1$) are real-valued on the imaginary k-axis. Moreover, from the expression (2.11), one can prove that there is a vicinity of $k = 0$ where $R(k)$ is also real-valued on the imaginary k-axis. Then equation (2.13) has a solution $T(t_n)$ modulo $2\pi/R$ in the region where $R(k)$ is real-valued. To express these solutions, we write

$$\tan\sigma = \frac{2\mathrm{i}kR}{H - 4k^2G} \tag{2.14}$$

and calculate the times t_n when these poles 'cross' the real axis by

$$RT(t_n) = -2\sigma + 2\pi n. \tag{2.15}$$

Moreover, the poles 'cross' the real axis in $k = 0$ for which one can prove that $\sigma = 0$. Hence the above equation becomes

$$T(t_n) = \frac{2\pi n}{R(0)} \tag{2.16}$$

where the value of $R(0)$ is obtained by using the bounds (2.19) below. An explicit solution will be obtained for a particular choice of the distribution $g(k)$ and input data in the next section.

From the unitarity relation [7, 11]

$$k \in \mathbb{R} : |\rho|^2 + |\tau|^2 = 1 \tag{2.17}$$

$\rho(k, t)$ cannot have poles on the real axis. Moreover, from expression (2.9) we can demonstrate that

$$t > 0 : \rho(0, t) = 1. \tag{2.18}$$

(With respect to [11], their definition of the reflection coefficient is $-\rho$.) The calculation proceeds by estimating the behaviours of $G(k)$ and $H(k)$ as $k \to 0$. We obtain

$$\begin{aligned} G(0) &= \lim_{h\to 0} \frac{1}{4} \int \mathrm{d}\lambda \, \frac{|g(\lambda)|^2}{\lambda^2 + h^2} \\ H(0) &= \frac{\gamma^2 - 1}{\gamma^2} \lim_{h\to 0} \frac{1}{2} \int \mathrm{d}\lambda \, \frac{\lambda^2 |g(\lambda)|^2}{\lambda^2 + h^2}. \end{aligned} \tag{2.19}$$

These are bounded values when $g(k)$ is $L^2(\mathbb{R})$ and behave as $\mathcal{O}(k)$ at the origin.

For the value $t = t_n$ the function $\rho(k, t_n)$ can be seen as a discontinuous function of k in $k = 0$. This can be seen in figure 1 where for $t = t_1$ the real part of $\rho(k, t_1)$ indeed looks discontinuous in zero. We have checked in this figure that Im (ρ) does vanish in $k = 0$ while it is also discontinuous for $t = t_n$. The very signature of a soliton creation is the fact that $\rho(k, t_n)$ does not go to 1 as $k \to 0$ (while $\rho(k, t_n + 0)$ and $\rho(k, t_n - 0)$ do).

The eight parts of figure 1 actually represent the real and imaginary parts of $\rho(k, t)$ as functions of k for different times before, during and after a soliton birth, for a choice of boundary values and distribution $g(k)$ given next.

Equation (2.16) shows that, when the system has constant boundary values, it *periodically* produces solitons. Moreover, if the input vanishes for $t > t_m$, ρ will no longer depend on t and the created solitons are frozen in the medium for $t > t_m$. Hence, for a finite-duration input, we can infer the total number of solitons created by the interaction of the wave field u with the medium q. We discuss this in more detail in the next section where we choose a particular distribution $g(k)$ and compare the result with numerical integration of the model on the finite interval.

3. Soliton generation: numerical simulations

The purpose of this section is to compare the solution obtained by IST in the preceding section to numerical simulations of the system (2.1) with initial datum $q(x, 0) = 0$ and boundary values (2.8) with the choice

$$g(k) = \frac{k}{\sqrt{1 + k^4}} \qquad a(t) = 1 \qquad \gamma = 0.5. \tag{3.1}$$

Such a comparison begins by getting from the (numerical) solution of (2.1) the output field value expressed as

$$\begin{aligned} u(k, x, t)|_{x=L} &= U_e(k, t)\mathrm{e}^{\mathrm{i}kL} + V_e(k, t)\mathrm{e}^{-\mathrm{i}kL} \\ u_x(k, x, t)|_{x=L} &= \mathrm{i}kU_e(k, t)\mathrm{e}^{\mathrm{i}kL} - \mathrm{i}kV_e(k, t)\mathrm{e}^{-\mathrm{i}kL} \end{aligned} \tag{3.2}$$

which allows us to extract the functions $U_e(k, t)$ and $V_e(k, t)$. Then an 'experimental' spectral transform $\rho_e(k, t)$ is constructed by analogy with expression (2.5) as

$$\rho_e(k, t) = -\frac{\overline{V_e}(k, t)B(k, t) - U_e(k, t)\overline{A}(k, t)}{\overline{V_e}(k, t)A(k, t) - U_e(k, t)\overline{B}(k, t)}. \tag{3.3}$$

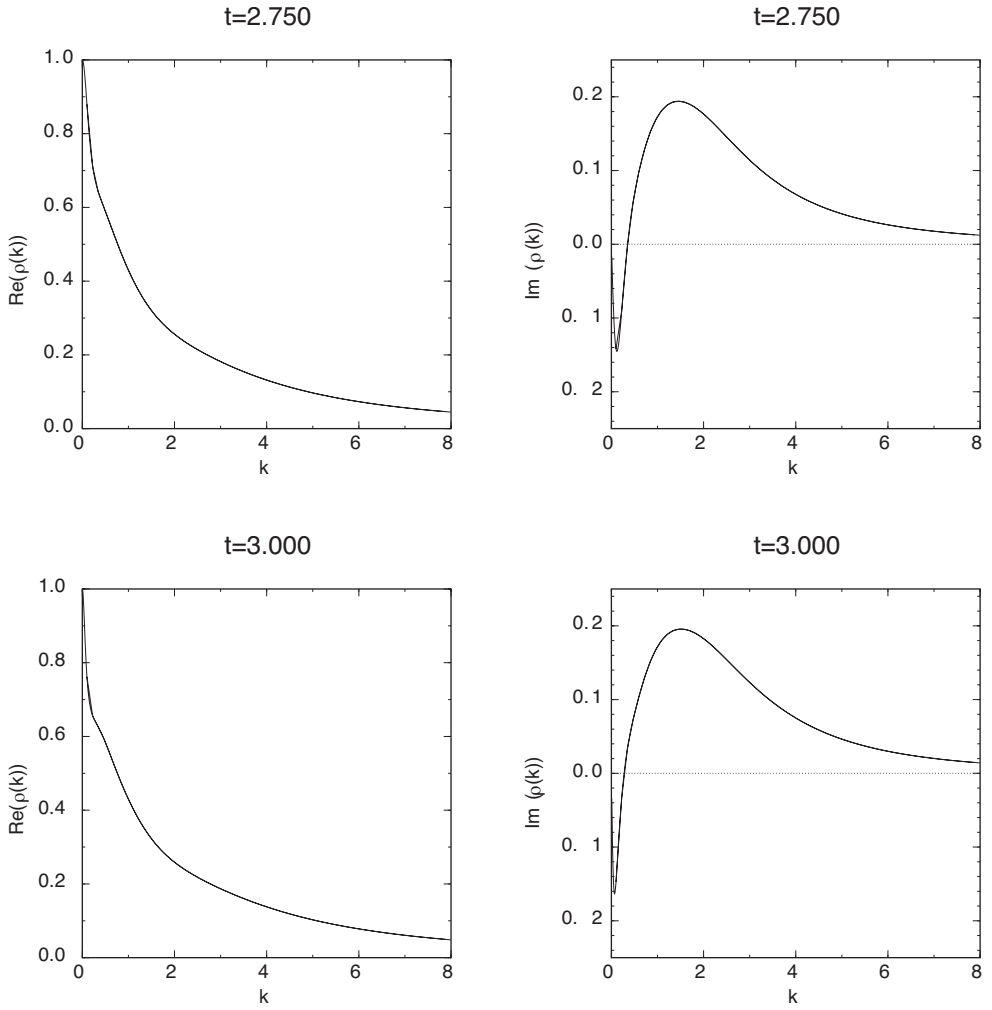

Figure 1. Plots of real and imaginary parts of the function $\rho(k)$ at different times about the value $t = 3.26$ of the soliton creation. Each graph contains both a theoretical and numerical curve which are so close to each other (relative difference less that 10^{-3}) as to be indistinguishable. (Continued on next page.)

This value is now compared with the theoretical expression (2.9) written in the case (3.1) obtained by computing $H(k)$ and $G(k)$. By the residue theorem we get

$$\begin{aligned} H(k) &= \frac{1-\gamma^2}{\gamma^2}\frac{\pi\sqrt{2}}{4}\frac{\mathrm{i}\sqrt{2}k+1}{(k-\zeta)(k+\bar{\zeta})} \\ G(k) &= -\frac{\pi\sqrt{2}}{8}\frac{1}{(k-\zeta)(k+\bar{\zeta})} \qquad \zeta = \sqrt{2}/2(\mathrm{i}-1) \end{aligned} \tag{3.4}$$

from which the explicit expression (2.9) of $\rho(k,t)$ follows. This is compared with (3.3) and the result is shown in figure 1.

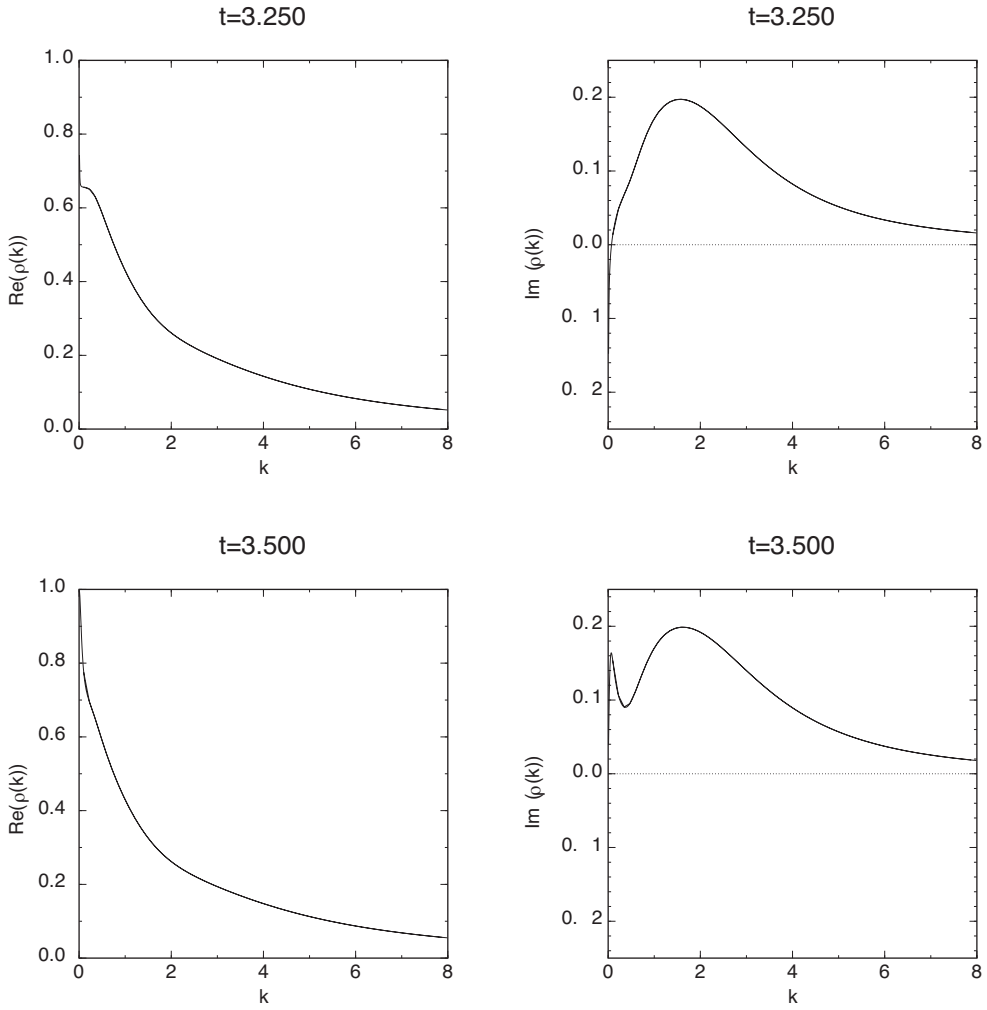

Figure 1. (Continued)

Note, first, that from formula (2.16) we have

$$T(t_n) = 4n\gamma\sqrt{\frac{2}{1-\gamma^2}} \tag{3.5}$$

and, consequently, for the choice (3.1) the creation of the first soliton occurs at $t_1 = 3.26$. We have plotted in each graph both the theoretical value (2.9) and the 'experimental' expression (3.3) obtained by solving numerically the system (2.1) on a finite length $L = 32$. The curves coincide in a striking manner: we have estimated the relative discrepancy which never exceeds 10^{-3} for $k \in [0.1, 8.0]$. We have thus demonstrated that ρ_e provides us with a very accurate and efficient tool to analyse the solution of (2.1). This tool, namely the formula (3.3), can therefore be used for any numerical simulation, even when it has no explicit theoretical counterpart to compare with.

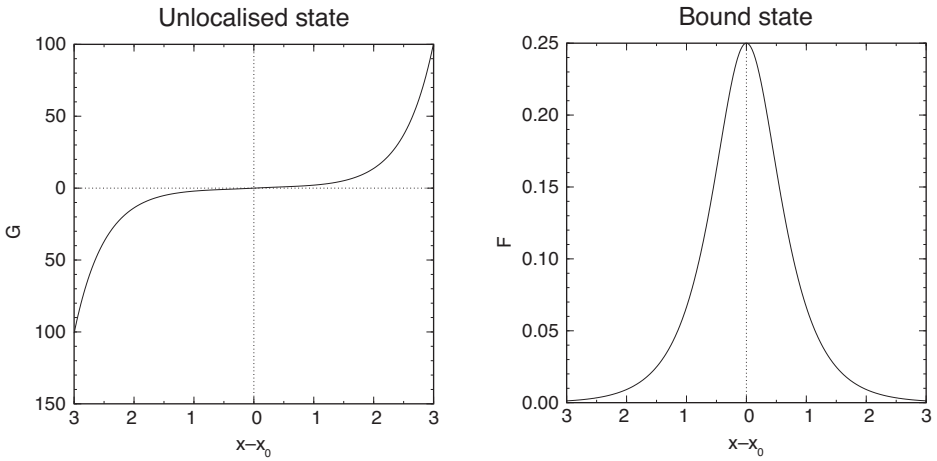

Figure 2. Bound state and unlocalized state in a solitonic potential.

4. Driving the soliton

The model (1.8) introduced in [9] was at the origin of the conjecture that ion-sound waves in plasmas can generate energy transmission at a frequency below the plasma frequency by means of soliton creation. We have just demonstrated that this is indeed the case. Now we want to show that the arbitrariness of the boundary values allows one to drive the soliton.

The method used consists in assuming a sech-shape pulse for the potential (ion-sound wave) $q(x,t)$ and then expressing the related electric field u as a linear superposition of the two eigenfunctions of the Schrödinger spectral problem (with the negative eigenvalue related to the particular choice of q).

For the eigenvalue $k^2 = -\delta^2$, we take

$$q(x,t) = \frac{-2\delta^2}{\cosh^2(\delta(x - x_0))} \tag{4.1}$$

where $x_0(t)$ is the (time-dependent) *unknown* pulse position. The two eigenfunctions are the usual bound-state eigenfunction

$$F(x,t) = \frac{1}{\cosh(\delta(x - x_0))} \tag{4.2}$$

and the unbounded eigenfunction

$$G(x,t) = \frac{1}{4}\frac{\sinh(2\delta(x - x_0)) + 2\delta(x - x_0)}{\cosh(\delta(x - x_0))}. \tag{4.3}$$

The moduli of these two solutions are shown in figure 2.

Then the solution $u(x,t)$ is sought as the linear combination

$$u(x,t) = \alpha(t)F(x,t) + \beta(t)G(x,t) \tag{4.4}$$

and the game consists in finding α and β in terms of $x_0(t)$, which then will allow us to compute the pulse velocity $v = \dot{x}_0$ via the evaluation of the height of the electric pulse $u(x,t)$. This is done by using the nonlinear rule (note that, for $\beta = 0$, α is the maximum value of $u(x,t)$)

$$v(t) = \frac{\alpha(t)}{4\delta^2} \tag{4.5}$$

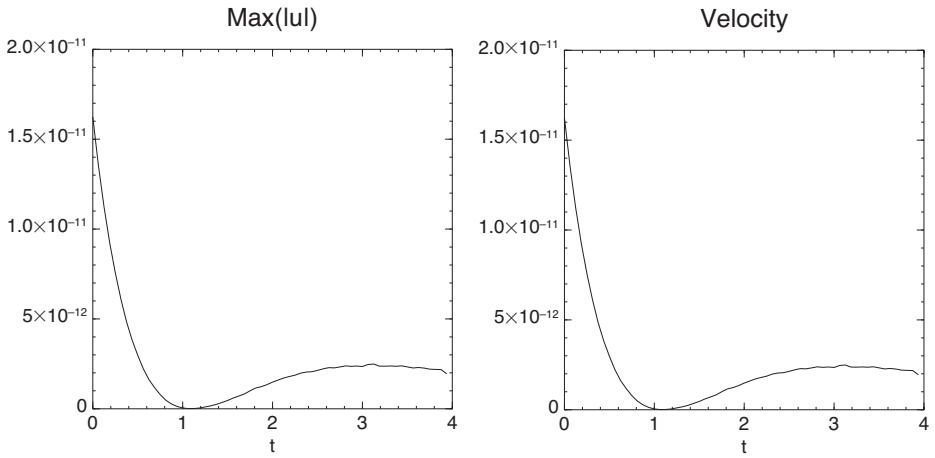

Figure 3. The velocity of the soliton, and the squared value of the maximum of the bound state. Theoretical curves and numerical ones are indistinguishable. These graphs have been calculated with an interval of length 20 and parameter $\delta = 1$.

which holds for exact soliton solution of the full-line case (for which $\beta = 0$ necessarily). This gives, in general, an approximate result—except if $\beta = 0$ for all t. We will show with numerical simulations that this approximation is quite good.

From the boundary values (1.9) we obtain

$$\alpha(t) = -\frac{a(t)}{2\cosh(\delta x_0)}[1 + \delta x_0 + \cosh^2(\delta x_0)] - \frac{b(t)}{4\delta\cosh(\delta x_0)}[\sinh(2\delta x_0) + 4\delta x_0\cosh(\delta x_0)]. \tag{4.6}$$

The system of equations (4.5), (4.6) is a first-order nonlinear differential equation for the unknown $x_0(t)$. It is solved numerically and we show an example in figure 3 where, in particular, we compare the obtained velocity to the measure of the maximum value of $u^2(x, t)$ at each time, which justifies, for that choice, the nonlinear rule (4.5).

The program used to verify these results uses standard methods of finite differences and interpolation from [12] or [13]. It takes an arbitrary chosen initial condition and two boundary conditions at one end and allows the initial condition to evolve. The numerical schemes are the Runge–Kutta–Fehlberg method on an equispaced grid to solve at each time the value of $u(x, t)$, for all x in its potential $q(x, t)$, and a simple Runge–Kutta method to find the potential at the next time $(t + \mathrm{d}t)$ for each time t.

Appendix A. Evolution of the spectral transform

The output solution

$$u(k, x, t)|_{x\to\infty} \sim U(k, t)\mathrm{e}^{\mathrm{i}kx} + V(k, t)\mathrm{e}^{-\mathrm{i}kx} \tag{A.1}$$

of the Karpman–Kaup system (2.1) has been shown in [7] to be given by

$$U = \frac{1}{\tau}(B + A\rho) \qquad V = \frac{1}{\overline{\tau}}(A + B\overline{\rho}) \tag{A.2}$$

with $A(k, t)$ and $B(k, t)$ given in (2.7). Note that the above linear system can be inverted to get the expression (2.5) of $\rho(k, t)$ in terms of the (given) input data $A(k, t)$, $B(k, t)$ and the

(measured or calculated) output $U(k,t)$, $V(k,t)$. This is possible if $|A| \neq |B|$ which requires some linear independence of the inputs. An explicit example in the case $|A| = |B|$ has been treated in [7]. The function $\tau(k,t)$, called the transmission coefficient, can be obtained either from ρ or else by solving the linear system (A.2), but its expression is not required for our purpose.

From now on we restrict ourselves to the case (2.8), that is, to

$$A(k,t) = \tfrac{1}{2}(1-\gamma)g(k)a(t) \qquad B(k,t) = \tfrac{1}{2}(1+\gamma)g(k)a(t). \tag{A.3}$$

The function $\rho(k,t)$ is the spectral transform obtained by solving a Riccati time evolution given in [7], which in the example chosen above reduces to[2]

$$\partial_t \rho = a(t)^2 \left[\frac{H}{4\mathrm{i}k}(1-\rho)^2 - 2\mathrm{i}kG\rho \right] \tag{A.4}$$

where the functions $G(k)$ and $H(k)$ are as defined in (2.10). This equation can then be linearized and solved by using standard methods and, in the new *time* variable T defined in (2.12), this equation reads

$$\frac{\partial \rho}{\partial T} = \frac{H}{4\mathrm{i}k}(1-\rho)^2 - 2\mathrm{i}kG\rho. \tag{A.5}$$

The solution of the above evolution for the initial condition

$$\rho(k,0) = 0 \tag{A.6}$$

corresponding to $q(x,0) = 0$, i.e. to a medium initially at rest, is written in (2.9).

Appendix B. Solution on the finite interval

The spectral transform given in [7] on the semi-line $x > 0$ can be used to solve the finite-interval problem $x \in [0, L]$ for the boundary values $u(k,0,t)$ and $u_x(k,0,t)$ and initial datum $q(x,0)$ in the following way:

(1) Construct the spectral transform $\rho(k,0)$ from initial datum $q(x,0)$ by prolongating it to zero for $x > L$ (note that we always take $q(x,0) = 0$).
(2) Solve the Riccati time evolution (A.4) of ρ (or the more general one in [7]) with initial datum $\rho(k,0)$.
(3) Reconstruct the solution $u(k,x,t)$ for any value of x (in particular in the interval $x \in [0, L]$) by first solving the system of linear integral equations (k_n are the N positions of the poles of $\rho(k,t)$ in the lower half-plane)

$$\begin{aligned}\phi(k,x,t) = 1 &+ \frac{1}{2\mathrm{i}\pi}\int_{-\infty}^{+\infty} \frac{\mathrm{d}\lambda}{\lambda - k - \mathrm{i}0}\phi^+(-\lambda,x,t)\rho(\lambda,t)\mathrm{e}^{2\mathrm{i}\lambda x} \\ &+ \sum_{n=1}^{N} \frac{1}{k_n - k}\phi^+(-k_n,x,t)\operatorname*{Res}_{k_n}\{\rho(k,t)\}\mathrm{e}^{2\mathrm{i}k_n x}\end{aligned} \tag{B.1}$$

and then by using

$$u(k,x,t) = A(k,t)\phi^+(k,x,t)\mathrm{e}^{-\mathrm{i}kx} + B(k,t)\phi^+(-k,x,t)\mathrm{e}^{\mathrm{i}kx}. \tag{B.2}$$

Finally, the potential is reconstructed by

$$q(x,t) = -2\mathrm{i}\partial_x \phi^{(1)}(x,t) \tag{B.3}$$

where $\phi^{(1)}$ denote the coefficient of $1/k$ of the Laurent series of $\phi(k)$.

[2] For the case (2.1) considered here, one should discard the term $-2\mathrm{i}k\rho$ in the evolution (4.18) of [7].

References

[1] Goldman M V 1984 *Rev. Mod. Phys.* **56** 709
Laedke E W and Spatschek K H 1980 *Phys. Fluids* **23** 44
[2] Zakharov V E 1972 *Sov. Phys.–JETP* **35** 908
[3] Davydov A S 1985 *Solitons in Molecular Systems* (Dordrecht: Reidel)
[4] Takeno S 1985 *Prog. Theor. Phys. Lett.* **73** 853
[5] Yariv A 1975 *Quantum Electronics* (New York: Wiley)
[6] Benney D J 1977 *Stud. Appl. Math.* **56** 81
[7] Hugot F-X and Leon J 1999 *Inverse Problems* **15** 701
[8] Barthes M, Leon J and Spire A 2000 Nonlinearité dans les chaînes á liaison hydrogéne *Proc. Rencontres du Non-lineaire (Paris, 2000)* vol 50 168 (Paris: Onze Editions)
[9] Karpman V I 1975 *Phys. Scr.* **11** 263
[10] Kaup D J 1987 *Phys. Rev. Lett.* **59** 2063
[11] Chadan K and Sabatier P C 1989 *Inverse Problems in Quantum Theory* (New York: Springer)
[12] Abramowitz M and Stegun I A 1970 *Handbook of Mathematical Functions* (New York: Dover)
[13] Press W H, Teukolsky S A, Vetterling W T and Flannery B P 1992 *Numerical Recipes in C* (Cambridge: Cambridge University Press)